Absolute Rate Constants in the Concerted Reduction of Olefins by Diazene

H. R. Tang, M. L. McKee, and D. M. Stanbury*

Contribution from the Department of Chemistry, Auburn University, Auburn, Alabama 36849

Received May 19, 1995[⊗]

Abstract: Absolute rate constants are reported for the reactions of aqueous 1,2-diazene with fumaric acid in its three states of protonation, as well as for the reaction with the maleate dianion. The acid hydrolysis of azodiformate was used as the source of diazene, which underwent competitive disproportionation and substrate hydrogenation. In one set of experiments the decay of diazene was monitored optically in a stopped-flow instrument; the rate constants were extracted from the increased decay rates arising from additions of the substrate. In the other set of experiments the product yields were determined by ^{1}H NMR spectroscopy; rate constants were derived from these yields by use of the known rate of disproportionation of diazene. The rate constants obtained are $(1.32 \pm 0.07) \times 10^2$ M^{-1} s^{-1} for fumaric acid, $(2.4 \pm 0.5) \times 10^2$ M^{-1} s^{-1} for the hydrogen fumarate anion, $(8.0 \pm 0.5) \times 10^2$ M^{-1} s^{-1} for the fumarate dianion, and 94.5 M^{-1} s^{-1} for the maleate dianion, all at 25 °C. Ab initio calculations on the reaction with the fumarate dianion show that these rate constants, although substantially smaller than for the disporportionation of diazene, are nevertheless in agreement with a synchronous concerted pericyclic double hydrogen atom transfer mechanism.

Introduction

1,2-Diazene, also known as diimide, N_2H_2, is widely used for reducing multiple bonds.[1] It is highly selective and stereospecific and has been in wide use since the early 1960s. An unusual feature of its chemistry is that diazene is believed to react through a pericyclic transition state, with both hydrogen atoms donating across the multiple bond. In recent experimental investigations we have measured the kinetics of diimide reduction of itself in aqueous media, i.e., its disproportionation.[2] We found that the rate law, rate constant, and activation parameters were in agreement with ab initio calculations based on the following scenario: (1) *trans*-N_2H_2 is in solvent-catalyzed equilibrium with its high-energy cis isomer, and (2) the cis isomer donates both hydrogen atoms in a concerted pericyclic manner with virtually no activation enthalpy, the transition state being highly entropy controlled. The ab initio calculations also indicated a very similar picture for the reduction of ethylene.[3] An interesting outcome of this computational study was the recognition that electron correlation must be taken into account in order to obtain a qualitatively correct picture of the potential energy surface: high activation energies rather than activationless reactions were obtained in prior computational studies of olefin hydrogenation by diazene and its disproportionation that omitted electron correlation.[4−9] The concept of solvent-catalyzed isomerization of diazene has subsequently been supported and refined in ab initio results reported by McKee.[10]

Experimental studies of the kinetics of diazene reductions of olefins have largely been limited to determining relative rates.[1] Thus, for example, it has been shown that fumaric acid is 10-fold more reactive than maleic acid.[11,12] On the basis of a large number of such measurements Garbisch et al. developed a predictive model in terms of strain energies.[13] Such a model might appear to be inconsistent with the entropy-controlled picture that we have developed, but a full assessment should be based on absolute rate constants rather than the relative ones heretofore considered. To our knowledge, the only absolute rate constants that have been reported for reactions of diazene with olefins are those of Willis et al. for gas-phase reactions.[14] In that report, however, it was inferred that isomerization of diazene was rate limiting, and so it is difficult for us to place much confidence in the derived hydrogenation rate constants. In the current paper we report some progress toward resolving these issues by presenting the first absolute rate constants for olefin hydrogenation by aqueous diazene. Since trans−cis isomerization of diazene is rapid in aqueous solution,[2] the rate constants measured are composites that include the hydrogenation step *per se*.

Experimental Section

Reagents. Potassium azodiformate, $K_2[(NCO_2)_2]$, was prepared from azodicarbonamide (Aldrich) in aqueous KOH, as described by Thiele.[15] Fumaric acid (*trans*-$C_2H_2(COOH)_2$) (Mallinckrodt), maleic acid (Aldrich), succinic acid (Aldrich), acetic acid glacial (Aldrich, 99.99+% purity), sodium hydroxide (Fisher, ACS certified), phosphoric acid (J. T. Baker Chemicals), and tartaric acid (Fisher) were used without further purification. Acetic-d_3 acid-*d*, sodium deuteroxide, deuterium oxide (99.996% atom D), and deuterium oxide (99.9 atom % D with 1% w/w DSS, DSS = $Me_3Si(CH_2)_3SO_3Na$) were used as supplied by

[⊗] Abstract published in *Advance ACS Abstracts*, August 1, 1995.

(1) Pasto, D. J.; Taylor, R. T. *Org. React.* **1991**, *40*, 91−155.
(2) Tang, H. R.; Stanbury, D. M. *Inorg. Chem.* **1994**, *33*, 1388−1391.
(3) McKee, M. L.; Squillacote, M. E.; Stanbury, D. M. *J. Phys. Chem.* **1992**, *96*, 3266−3272.
(4) Skancke, P. N. *Chem. Phys. Lett.* **1977**, *47*, 259−264.
(5) Flood, E.; Skancke, P. N. *Chem. Phys. Lett.* **1978**, *54*, 53−56.
(6) Pasto, D. J. *J. Am. Chem. Soc.* **1979**, *101*, 6852−6857.
(7) Pasto, D. J.; Chipman, D. M. *J. Am. Chem. Soc.* **1979**, *101*, 2290−2296.
(8) Agrafiotis, D. K.; Rzepa, H. S. *J. Chem. Soc., Chem. Commun.* **1987**, 902−904.
(9) Agrafiotis, D. K.; Rzepa, H. S. *J. Chem. Soc., Perkin Trans. 2* **1989**, 475−488.
(10) McKee, M. L. *J. Phys. Chem.* **1993**, *97*, 13608−13614.
(11) Hünig, S.; Müller, H. R. *Angew. Chem., Int. Ed. Engl.* **1962**, *1*, 213−214.
(12) Hünig, S.; Müller, H. R.; Thier, W. *Angew. Chem., Int. Ed. Engl.* **1965**, *4*, 271−280.
(13) Garbisch, E. W., Jr.; Schildcrout, S. M.; Patterson, D. B.; Sprecher, C. M. *J. Am. Chem. Soc.* **1965**, *87*, 2932−2944.
(14) Willis, C.; Back, R. A.; Parsons, J. M.; Purdon, J. G. *J. Am. Chem. Soc.* **1977**, *99*, 4451−4456.
(15) Thiele, J. *Liebigs Ann. Chem.* **1892**, *271*, 127−137.

0002-7863/95/1517-8967$09.00/0

Aldrich. Distilled deionized water was obtained by passage of deionized water through a Barnstead pretreatment cartridge and subsequent distillation in a Barnstead Fi-streem all-glass still.

Methods. Solutions of azodiformate were prepared in aqueous 0.2 M NaOH or 0.2 M NaOD in D_2O. The initial concentrations of azodiformate were determined from the absorbance of the azodiformate stock solution at 402 nm on a Hewlett-Packard 8452A spectrophotometer, 2 nm resolution, with quartz cells of 1.00 cm path length. This analysis used a value of 33 M^{-1} cm^{-1} for the molar absorptivity of azodiformate.[16]

Solution pH values were measured at room temperature with a Corning 130 pH meter equipped with a combination electrode (Corning No. 476541) filled with saturated NaCl.

The UV spectrum of N_2H_2 was obtained on a OLIS RSM-1000 model rapid scanning stopped-flow spectrophotometer. This instrument obtains one scan per ms at 1 nm resolution, with a quartz cell of 1.7-cm path length. An alkaline solution of azodiformate was mixed in the stopped flow with an acetic acid solution so as to generate a mixture at pH 4.6. Under these conditions the azodiformate decays within the dead time of the instrument, generating N_2H_2 quantitatively.[2] The subsequent decay of the N_2H_2 was recorded and fit to a homogeneous second order decay with Global Analysis. This OLIS-supplied routine simultaneously fits the decay at all wavelengths and generates a spectrum of the absorbing species.

The kinetics studies were performed on a Hi-Tech Scientific Model SF-51 stopped-flow apparatus equipped with a SU-40 spectrophotometer and a C-400 circulating water bath that maintained the temperature of the cell compartment at 25 ± 0.1 °C. In all cases there was at least a 10-fold excess of fumaric acid over diazene. An OLIS 4300S system was used for data acquisition and analysis. Reactions were monitored in the 1 cm path length configuration at 360 nm, and the rate constants were obtained by fitting the data with OLIS-supplied homogeneous second order and competing first and second order decay functions.

The products of reaction in deuterated media were obtained by mixing reactants, NaOD/D_2O solutions of azodiformate and DOAc/D_2O solutions of fumaric acid, in a one-to-one ratio in a N_2-filled glovebag at room temperature. The products of reaction in aqueous solution were collected from the exhaust syringe on the stopped-flow instrument after mixing reactants in a one-to-one ratio in the stopped-flow mixing chamber. The samples for ^1H NMR study were prepared by taking the product solutions to dryness in a vacuum desiccator and then dissolving them in D_2O under nitrogen gas in a glovebag.

^1H NMR spectra of reactant and product solutions were determined with a Bruker AC 250 spectrometer. They were run in D_2O solution with all shifts reported (in ppm) downfield from DSS. Integrals were performed with considerable care, and the method was checked with a standard mixture of succinic and fumaric acids.

The various reactions were performed with no background electrolyte. As a consequence the ionic strength varied as a function of buffer and substrate concentration; in general, however, it stayed within the range from 0.14 to 0.35 M.

Numerical Methods. A modified version of the Los Alamos nonlinear least-squares program[17] running on a Macintosh II computer was used to fit the pH dependence for the reduction of fumaric acid and its deprotonated forms. Real roots (k_{fum}) of the nonlinear functions that relate the product yields to the rate laws were obtained numerically by use of a bisection method.[18]

All ab initio calculations were performed with the GAUSSIAN 92 suite of programs.[19] Geometries were optimized at the HF/6-31G(d) and MP2/6-31G(d) levels. The base computational level is MP2-(FULL)/6-31G(d)//MP2/6-31G(d). Zero-point energies, thermal corrections, and entropies were evaluated using frequencies calculated at the HF/6-31G(d) level. Zero-point corrections were multiplied by a 0.90 factor. Hydration free energies were calculated by Cramer and Truhlar's AM1-SM2 method using fixed MP2/6-31G(d) geometries as described previously.[10]

(16) Stanbury, D. M. *Inorg. Chem.* **1991**, *30*, 1293−1296.
(17) Moore, R. H.; Zeigler, R. K. LSTSQR; Los Alamos National Laboratory: Los Alamos, NM, 1959.
(18) Russell, D. M. Mathview Professional; Brainpower, Inc., Agoura Hills, 1987.
(19) Frisch, M. J.; Trucks, G. W.; Head-Gordon, M.; Gill, P. M. W.; Wong, M. W.; Foresman, J. B.; Johnson, B. G.; Schlegel, H. B.; Robb, M. A.; Replogle, E. S.; Gomperts, R.; Andres, J. L.; Raghavachari, K.; Binkley, J. S.; Gonzalez, C.; Martin, R. L.; Fox, D. J.; DeFrees, D. J.; Baker, J.; Stewart, J. J. P.; Pople, J. A. Gaussian 92; Pittsburgh, PA, 1992.

Reaction Mechanism and Derivations

It is now well-established that reactions of aqueous diazene can be conducted by use of the acid-assisted hydrolysis of azodiformate;[20] the diazene so generated then reacts via competitive disproportionation and hydrogenation of the substrate.[1,16] This general mechanism is presented in Scheme 1, where fum and succ represent fumaric acid and succinic acid, respectively, with no implications as to their states of protonation.

Scheme 1

$$(NCO_2)_2^{2-} + 2H^+ \rightarrow N_2H_2 + 2CO_2 \quad k_0 \qquad \text{(R1)}$$

$$N_2H_2 + N_2H_2 \rightarrow N_2H_4 + N_2 \quad k_{disp} \qquad \text{(R2)}$$

$$N_2H_2 + \text{fum} \rightarrow \text{succ} + N_2 \quad k_{fum} \qquad \text{(R3)}$$

Because the rate of hydrolysis of azodiformate is first order with respect to $[H^+]$, qualitatively different types of behavior can be obtained depending on pH. Specifically, in acid solution the hydrolysis can occur so rapidly that diazene is generated quantitatively prior to its decay processes, while in alkaline solution the hydrolysis can be slow enough that the concentration of diazene never accumulates and it can be treated by the steady-state approximation. Moreover, it is possible to obtain the rate constants either by analysis of the time-dependent kinetics or the product yields. In the remainder if this section we present the derivations in the limiting acid regime for the kinetic method and in both limiting regimes for the yield-based methods. The derivations are given for the specific case where fumaric acid is the substrate, but they apply equally when the substrate is maleic acid.

The complete rate law for the variation of diazene concentration with time is

$$d[N_2H_2]/dt = k_0[H^+][(NCO_2)_2^{2-}] - k_{fum}[fum][N_2H_2] - 2k_{disp}[N_2H_2]^2 \quad (1)$$

where [fum] represents the total concentration of fumaric acid, irrespective of its state of protonation. As has been shown previously, the concentration of $(NCO_2)_2^{2-}$ is given by $[(NCO_2)_2^{2-}]_0e^{-k_0[H^+]t}$, with $k_0 = 1.8 \times 10^8$ M^{-1} s^{-1}.[16] Moreover, the reactions are well-buffered and conducted with a large excess of fumaric acid, so we can let $k_0[H^+] = k_0'$ and $k_{fum}[fum] = k'_{fum}$. These substitutions in eq 1 lead to

$$d[N_2H_2]/dt = k_0'[(NCO_2)_2^{2-}]_0e^{-k_0't} - k'_{fum}[N_2H_2] - 2k_{disp}[N_2H_2]^2 \quad (2)$$

The first term in the right-hand side of eq 2 depends on $[H^+]$ and time, such that it can be neglected at sufficiently long times at low pH, which leads to

$$-d[N_2H_2]/dt = k'_{fum}[N_2H_2] + 2k_{disp}[N_2H_2]^2 \quad (3)$$

I.e., at sufficiently low pH, N_2H_2 is generated essentially instantly and then undergoes decay by competitive pseudo-first-order hydrogenation and homogeneous second-order disproportionation (reactions R2 and R3). This is in agreement with

(20) Back, R. A. *Rev. Chem. Intermed.* **1984**, *5*, 293−323.

our previous report that at low pH (pH <6) the reaction of N_2H_2 with azobenzene-4,4′-disulfonate can be treated analogously.[16]

Under all conditions, the overall rate law for the formation of succinic acid is expressed as

$$d[succ]/dt = k'_{fum}[N_2H_2] \quad (4)$$

At low pH the concentration of N_2H_2 is given by the integral of eq 3, which is

$$[N_2H_2] = \frac{k'_{fum}}{\left(\frac{k'_{fum}}{[N_2H_2]_0} + 2k_{disp}\right)e^{k'_{fum}t} - 2k_{disp}} \quad (5)$$

Substituting this result into eq 4 leads to

$$[succ] - [succ]_0 = \frac{k'_{fum}}{2k_{disp}} \ln\left(1 + \frac{2k_{disp}[N_2H_2]_0}{k'_{fum}} - \frac{2k_{disp}[N_2H_2]_0}{k'_{fum}e^{k'_{fum}t}}\right) \quad (6)$$

which, at $t = \infty$ becomes

$$[succ]_\infty - [succ]_0 = \frac{k'_{fum}}{2k_{disp}} \ln\left(1 + \frac{2k_{disp}[N_2H_2]_0}{k'_{fum}}\right) \quad (7)$$

Equations 3 and 7 are thus the ones to be used in analyzing the kinetics and product yields under conditions of low pH.

On the other hand, at high pH, the first term in the right-hand side of eq 2 becomes rate-limiting and cannot be ignored. Under these conditions the rapid reactions that consume N_2H_2 cause its concentration never to accumulate. Its concentration is obtained by applying the steady-state approximation to the concentration of N_2H_2 in eq 2, which leads to

$$[N_2H_2]_{ss} = \frac{-k'_{fum} + \sqrt{(k'_{fum})^2 + 8k_{disp}k_0'[(NCO_2)_2^{2-}]_0 e^{-k_0't}}}{4k_{disp}} \quad (8)$$

If eq 4 is integrated with this definition of $[N_2H_2]$, the result is

$$[succ]_\infty - [succ]_0 = \frac{k'_{fum}}{2k_{disp}k_0'}(B - k'_{fum}) - \frac{(k'_{fum})^2}{2k_{disp}k_0'}[\ln(B + k'_{fum}) - \ln(2k'_{fum})] \quad (9)$$

where $B = \{(k'_{fum})^2 + 8k_{disp}[(NCO_2)_2^{2-}]_0k_0'\}^{1/2}$. Eq 9 permits rate constants to be evaluated from product analyses under conditions of high pH.

Although not indicated specifically in Scheme 1, fumaric acid is a diprotic acid. As a consequence, the values of k_{fum} obtained by use of the above equations are conditional rate constants. If it is assumed that each of the states of protonation (designated H_2fum, $Hfum^-$, and fum^{2-}) have characteristic rate constants for their reactions with N_2H_2, the appropriate expression is

$$k'_{fum} = k_{fum}[fum] = k_1[H_2fum] + k_2[Hfum^-] + k_3[fum^{2-}] \quad (10)$$

If the successive acid dissociation constants of H_2fum are given as K_{a1} and K_{a2}, then the individual concentrations are given by $[Hfum^-] = K_{a1}[H_2fum]/[H^+]$, and $[fum^{2-}] = K_{a1}K_{a2}[H_2fum]/[H^+]^2$, and the total concentration of fumaric acid is given by

$$[fum] = \left(1 + \frac{K_{a1}}{[H^+]} + \frac{K_{a1}K_{a2}}{[H^+]^2}\right)[H_2fum] \quad (11)$$

These considerations lead to a pH dependence for k_{fum} as shown by eq 12:

$$\frac{k'_{fum}}{[fum]} = k_{fum} = \frac{k_1 + \frac{k_2K_{a1}}{[H^+]} + \frac{k_3K_{a1}K_{a2}}{[H^+]^2}}{1 + \frac{K_{a1}}{[H^+]} + \frac{K_{a1}K_{a2}}{[H^+]^2}} \quad (12)$$

Results

In previous work we reported that diazene could be generated in the dead time of our stopped-flow instrument (a few milliseconds) by mixing an alkaline solution of azodiformate with a solution of acetic (or other) acid.[2] We found that the diazene so generated could be detected by its absorption in the UV, and thereby its decay could be monitored. By repeating the experiment at various monitoring wavelengths we obtained the UV spectrum of aqueous diazene at low (~15 nm) resolution.[2] Our recent acquisition of a rapid-scanning stopped-flow instrument has enabled us to obtain spectra of such transients at the considerably higher resolution of 1 nm. The spectrum of N_2H_2 so obtained (Figure 1) is in agreement with that reported previously, and it shows that the vibronic fine structure, seen in the gas phase,[21] is completely obscured by solution-induced broadening.

The products of the reduction of fumaric acid by diazene (N_2H_2) and deuterated diazene (N_2D_2) were determined by ^1H NMR spectroscopy. The deuterated product solution clearly reveals a resonance for dideuteriosuccinic acid at 2.50 ppm downfield from DSS standard (see Figure 2). The corresponding nondeuterated reaction yields a resonance at 2.42 ppm for succinic acid. Reduction of maleic acid by N_2H_2 likewise yields a spectrum characteristic of succinic acid. The ^1H NMR spectra implicate a two-proton transfer to the unsaturated bond of fumaric acid or maleic acid as follows:

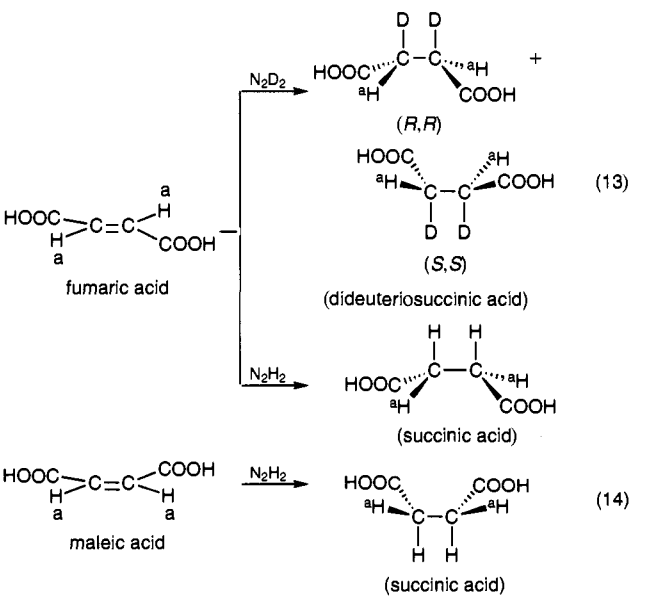

(13) (14)

These results are in agreement with the observations by Corey, Pasto and Mock.[22]

(21) Back, R. A.; Willis, C.; Ramsay, D. A. *Can. J. Chem.* **1978**, *56*, 1575–1578.

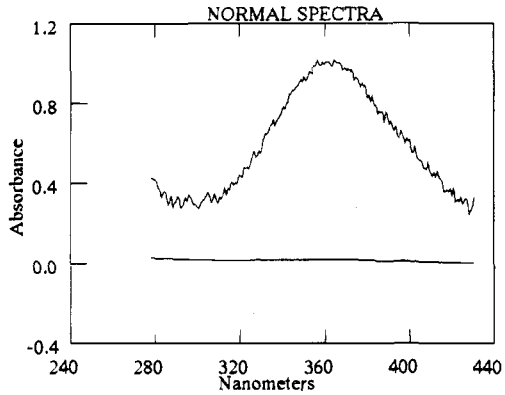

Figure 1. Solution phase spectrum of N_2H_2 at 1 nm resolution. Spectrum obtained from global fit of 3-D data at 25 °C, 0.3 M ionic strength, and pH 4.6 with $[N_2H_2]_0 = 1.91$ mM, [NaOH] = 0.1 M, and [HOAc] = 0.21 M.

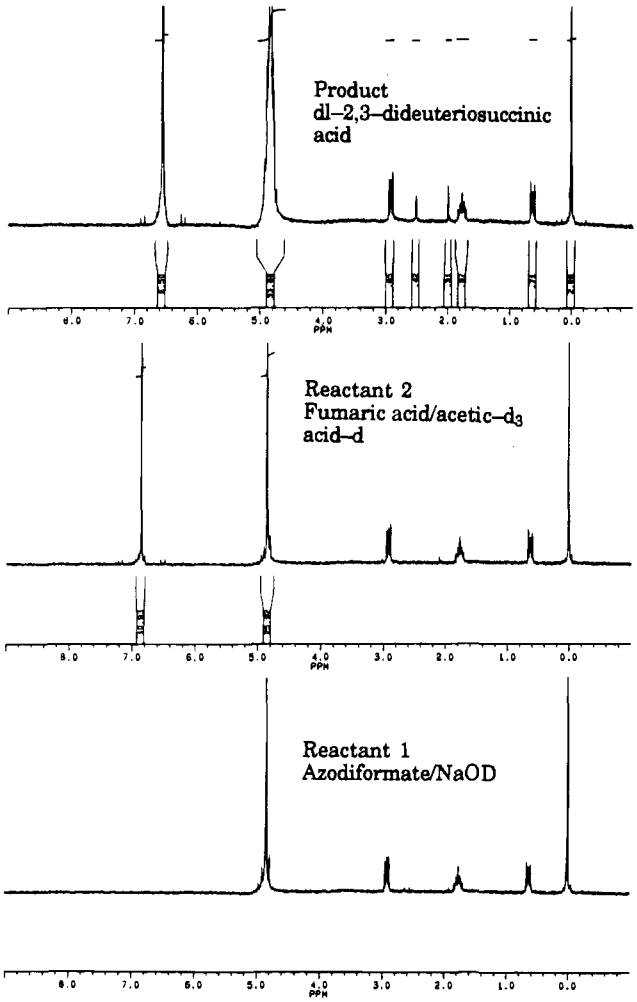

Figure 2. ^{1}H NMR spectra of hydrogenation of fumaric acid by N_2D_2. pH = 4.4, [fumaric acid] = 20 mM, and $[N_2D_2]_0 = 2.57$ mM. Ionic strength = 0.2 M.

Comparison of the integrated aliphatic ^{1}H NMR peak intensity of dideuteriosuccinic acid (δ 2.50 ppm) with that of fumaric acid (δ 6.54 ppm) (Figure 2) indicates that less than 7% of the fumaric acid is converted into succinic acid. However, quantitative conversion in this experiment would have given a 10% yield. Similar less-than-quantitative yields were found in a series of 11 experiments spanning the range from pH 1 to 7,

Table 1. Product Yields and Rate Constants As Determined from ^{1}H NMR Spectra[a]

pH	I_{succ}/I_{fum}	[fum], mM	[succ], M	k_{fum}, $M^{-1}s^{-1}$
1.05[b]	1.98×10^{-2}	20.8	2.06×10^{-4}	1.23×10^2
1.24[b]	2.16×10^{-2}	20.8	2.26×10^{-4}	1.38×10^2
1.31[b]	2.08×10^{-2}	20.8	2.16×10^{-4}	1.31×10^2
1.41[b]	2.10×10^{-2}	20.9	2.20×10^{-4}	1.33×10^2
1.61[b]	2.20×10^{-2}	20.9	2.29×10^{-4}	1.42×10^2
2.56[b]	3.10×10^{-2}	21.0	3.26×10^{-4}	2.32×10^2
3.62[c]	3.65×10^{-2}	21.1	3.92×10^{-4}	3.11×10^2
4.34[c]	5.24×10^{-2}	21.1	5.63×10^{-4}	5.63×10^2
5.54[c]	6.25×10^{-2}	21.7	6.71×10^{-4}	7.73×10^2
6.74[d]	7.72×10^{-2}	21.8	8.30×10^{-4}	8.69×10^2
7.18[d]	1.03×10^{-1}	21.8	1.11×10^{-3}	8.59×10^2
pH	I_{succ}/I_{fum}	[mal], mM	[succ], M	k_{mal}, $M^{-1}s^{-1}$
6.07[d]	1.38×10^{-2}	21.5	1.49×10^{-4}	78.1
7.25[d]	2.12×10^{-2}	21.5	2.28×10^{-4}	94.5

[a] Reaction at 25 °C and $[(NCO_2)_2^{2-}]_0 = 1.23$ mM. [b] Perchlorate buffer. [c] Acetate buffer. [d] Phosphate buffer.

and they were also found in the experiments where maleic acid was used as the substrate (see Table 1). A quantitative treatment of these results is presented below, but qualitatively they can be accounted for by a mechanism involving competition between disproportionation and hydrogenation, as in

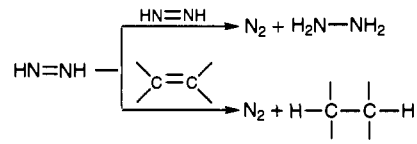

(15)

The existence of this type of competition was inferred by Hünig, Müller, and Thier in 1965 for reactions where N_2H_2 was generated by oxidation of N_2H_4 by $[Fe(CN)_6]^{3-}$,[12] but the current paper presents the first quantitative treatment of this phenomenon.

Initial studies of the kinetics of reduction of fumaric acid by N_2H_2 in protic buffers were performed by stopped-flow spectrophotometry. Solutions of fumaric acid (16.0–26.7 mM) prepared in acetate and tartarate buffers were mixed with azodiformate/sodium hydroxide solutions to generate mixtures at pH 4.39–4.23 and pH 3.05–2.98, respectively, with ionic strength between 0.14 and 0.25 M. This regrettably narrow range of fumaric acid concentrations was limited at the low end by the need for a significant kinetic contribution from the reaction with fumaric acid and at the high end by the solubility of fumaric acid (0.63 g in 100 g of water at 25 °C).[23] The decay of N_2H_2 was found to be dominated by the self-reaction of N_2H_2 and only mildly accelerated by the presence of fumaric acid. Ideally, the data would have been fitted with a function appropriate for competitive 1st- and 2nd-order decay, i.e.

$$A = \frac{1}{\frac{1}{A_0}e^{k'_{fum}t} + \frac{k'_{disp}}{k'_{fum}}(e^{k'_{fum}t} - 1)} + A_\infty \qquad (16)$$

which is the integrated form of eq 3 with $A = \epsilon b[N_2H_2]$, $A_0 = \epsilon b[N_2H_2]_0$, and $k'_{disp} = 2k_{disp}/\epsilon b$. However, in order to achieve numerical stability, the fits were conducted with k'_{disp} held equal to the value obtained by fitting the traces with a simple homogeneous second-order rate law under conditions of no added fumaric acid. Values of k'_{fum} and k'_{disp} as a function of the concentration of fumaric acid at the two pH values are given

(22) Corey, E. J.; Pasto, D. L.; Mock, W. L. *J. Am. Chem. Soc.* **1961**, *83*, 2957–2958.

(23) *The Merk Index*, 11th ed.; Budavari, S., Ed.; Merck & Co.: Rahway, NJ, 1989; p 671.

Table 2. Stopped-Flow Kinetics Data for the Reduction of Diazene by Fumaric Acid[a]

[fum], mM	k'_{fum}, s^{-1} pH 3.0[b]	k'_{fum}, s^{-1} pH 4.3[c]
16.0	5.38	7.84
18.7	6.02	9.04
21.4	7.00	10.2
24.4	8.16	11.6
26.7	8.79	13.0

[a] $[N_2H_2]_0 = 1.2$ mM, $\mu = 0.14-0.35$ M, ~23 °C. Values of k'_{fum} obtained by fitting eq 16 to the individual shots while holding k'_{disp} equal to the value obtained with [fum] = 0. [b] Tartrate buffer. $k'_{disp} = 1.91 \times 10^3$ s^{-1}. [c] Acetate buffer. $k'_{disp} = 1.86 \times 10^3$ s^{-1}.

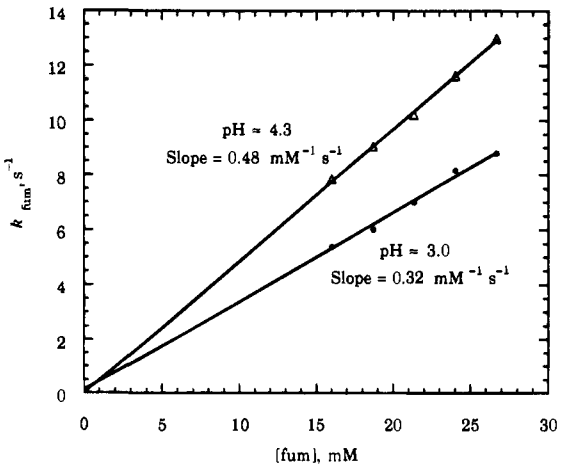

Figure 3. Pseudo-first-order rate constant dependence on the concentration of fumaric acid. $[N_2H_2]_0 = 1.2$ mM, ionic strength changes from 0.14 to 0.2 M. Open triangles at pH 4.23−4.39 with acetate buffer and solid circles at pH 2.98−3.05 with tartrate buffer.

in Table 2. The tabulated values of k'_{disp} are in good agreement with those reported previously.[2]

Plots of the pseudo-first-order rate constants, k'_{fum}, as a function of the concentration of fumaric acid at pH 4.3 and 3.0 gave excellent straight lines with zero intercepts (Figure 3). The second-order rate constant, k_{fum}, obtained from the slope of each line is 485 M^{-1} s^{-1} at pH 4.3 and 323 M^{-1} s^{-1} at pH 3.0. This mild pH dependence is not unexpected, since the fumaric acid undergoes deprotonation in this pH regime. More significantly, these results show that the second-order rate constant for the self-reaction of diazene is about two orders of magnitude greater than for its hydrogenation of fumaric acid.[2]

The above results, although significant, are not strictly unambiguous because of the small kinetic effect arising from the reaction with fumaric acid. Moreover, the stopped-flow method is limited to rather acidic conditions because of the need to generate N_2H_2 effectively instantly. These limitations can be overcome by the determination of quantitative product yields, described as follows. We measure the ratio of the integrated peak intensities for the ^1H NMR signals corresponding to the succinate and fumarate aliphatic protons, I_{succ}/I_{fum}. We then use the relationships [succ] = ([fum]/2) × (I_{succ}/I_{fum}) for reaction of N_2H_2, and [succ] = [fum] × (I_{succ}/I_{fum}) for reaction of N_2D_2, respectively. These relationships derive from the assumption that the integrated peak intensities are proportional to the proton concentrations, and the factor of $^1/_2$ disappears for the N_2D_2 reaction because the deuterons do not contribute to the signal. Analogous relationships apply to the reaction with maleic acid. Table 1 presents intensity ratios, I_{succ}/I_{fum}, for a series of reactions over the range from pH 1 to 7 for the reaction of N_2H_2 with fumaric acid and for a smaller range of pH for the corresponding reaction with maleic acid. The tabulated values

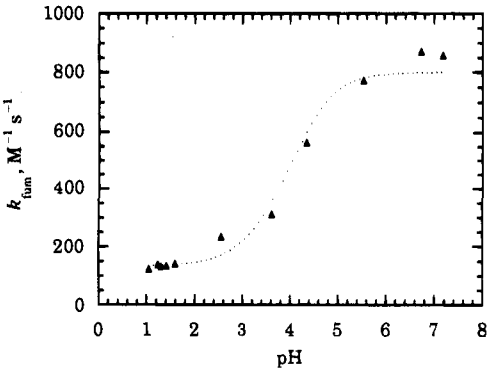

Figure 4. Plot of rate constant of reduction of fumaric acid by diazene as a function of pH. [fum] = 21.5 mM, $[N_2H_2]$ = 1.23 mM, pH = 1.05−7.18. Filled triangles are data from ^1H NMR experiments as shown in Table 1. Dotted curve is the least-squares fit.

of [succ] were derived from the intensity ratios by use of the above relationships under the approximation that the amount of substrate consumed was negligible.

Evaluation of the rate constants from the succinate yields requires use of eq 7 at low pH and eq 9 at high pH. Experimentally, we find that the half-life for decomposition of azodiformate is comparable to the half-life for loss of N_2H_2 at about pH 6. Thus we use eq 7 below pH 6 and eq 9 above pH 6.

To solve eqs 7 and 9 also requires accurate values for $[N_2H_2]_0$ and k_{disp}. Values of $[N_2H_2]_0$ were obtained from the measured absorbance of the stock solution of azodiformate under the assumption of quantitative conversion to N_2H_2 and the previously measured value of 33 M^{-1} cm^{-1} for ϵ_{400} for azodiformate.[16] The value of k_{disp} used in the calculations was taken from our prior publication: 2.2×10^4 M^{-1} s^{-1} for N_2H_2.[2] With these data in hand, eqs 7 and 9 were solved numerically to obtain values of k'_{fum}, which were then converted to the values of k_{fum} given in Table 1. In those cases where reasonable comparisons can be made, the results are in excellent agreement with those described above from the stopped-flow measurements.

Figure 4 illustrates the sigmoidal dependence of k_{fum} on pH. This pH dependence is interpreted to arise from the differing reactivity of fumaric acid and its mono- and di-deprotonated forms. Rate constants for the individual species were obtained by fitting eq 12 to these data along with the literature values of 1.16×10^{-3} and 8.3×10^{-5} M^{-1} for K_{a1} and K_{a2}, respectively, which were obtained from the tables of Smith and Martell after conversion to mixed stability constants and interpolation to 0.4 M ionic strength.[24] The best fit so obtained is shown in Figure 4, and the rate constants so obtained are $k_1 = (1.32 \pm 0.07) \times 10^2$ M^{-1} s^{-1}, $k_2 = (2.4 \pm 0.5) \times 10^2$ M^{-1} s^{-1}, and $k_3 = (8.0 \pm 0.5) \times 10^2$ M^{-1} s^{-1}. Although it might seem that these data should not define k_2 very precisely, this is not the case. If k_2 is set to zero a pronounced dip in the middle of the plot of k_{fum} vs pH is predicted, while values larger than optimal lead to a peak in the middle of the plot.

The value of k_{mal} obtained, 94.5 M^{-1} s^{-1} at pH 7.25, was not recorded as a function of pH. However, since the pH at which it was determined is in the region where maleic acid is fully deprotonated, this result should be analogous to the k_3 value obtained for the fumarate system. By use of measurements of relative yields Hünig et al. found that mal^{2-} was 10-fold less reactive than fum^{2-}, which is in good agreement with the ratio of 8.5 that we have found.[11,12]

(24) Smith, R. M.; Martell, A. E. *Critical Stability Constants*; Plenum: New York, 1989; Vol. 6, pp xv and 337.

An estimate of the deuterium kinetic isotope effect for k_{fum} was made by evaluating k_{fum} in D_2O by the NMR method described above. For the calculations it was assumed that ϵ_{400} for azodiformate was the same as in H_2O, and the value of k_{disp} used was taken from our prior publication: $6.7 \times 10^3\ M^{-1}\ s^{-1}$ for N_2D_2.[2] This led to a value for k_{fumD} of $2.93 \times 10^2\ M^{-1}\ s^{-1}$ at pH 4.4. Use of the corresponding value of k_{fum} from Table 1 gives a kinetic isotope effect of 1.9 at this pH. Since the reactions of all three states of protonation of fumaric acid contribute to the rates at this pH and each of them may have differing kinetic isotope effects, our measured kinetic isotope effect is necessarily a composite parameter.

Discussion

As described above, we have now determined the first solution-phase rate constants for hydrogenation of olefins by diazene, the specific olefins being fumaric acid, its mono- and dibasic forms, and the maleate dianion. To this list of substrates may be added the reactions of diazene with itself and with azobenzene-4,4′-disulfonate.[16] The trends to be noted are that diazene reacts fastest with itself, that increasing protonation of fumarate decreases the rates, and that its cis isomer, maleate, reacts more slowly.

It should be recognized that the predominant form of diazene in aqueous solution is believed to be the *trans*-1,2-isomer.[2] This is based on the characteristics of its UV spectrum and on ab initio calculations of the relative energies of the various isomers. However, it is also widely believed that the active form is the cis isomer because the stereospecificity of these reactions implies a pericyclic transition state. As in our prior report,[2] we propose a mechanism involving a rapid solvent-catalyzed cis−trans preequilibrium followed by rate-limiting double hydrogen atom transfer to the substrate. This mechanism is illustrated in Scheme 2 for fumarate as the substrate:

Scheme 2

$$trans\text{-}N_2H_2 \rightleftarrows cis\text{-}N_2H_2 \qquad K_{tc} \qquad \text{(R4)}$$

$$cis\text{-}N_2H_2 + fum^{2-} \rightarrow N_2 + succ^{2-} \qquad k_{2H} \qquad \text{(R5)}$$

According to this mechanism, the measured rate constant k_3 corresponds to the product $K_{tc}k_{2H}$. McKee has used a combined ab initio/AM1-SM2 solvation method to calculate a value of 4.9 ± 2.1 kcal/mol for $\Delta G°$ for reaction R4, which is equivalent to a value of -3.6 ± 1.5 for log K_{tc};[10] moreover, he has presented persuasive arguments that this isomerization can be very rapid due to acid catalysis by the solvent. His value for K_{tc} leads to values for k_{2H} of $5 \times 10^5\ M^{-1}\ s^{-1}$ for fumaric acid, $9 \times 10^5\ M^{-1}\ s^{-1}$ for $Hfum^-$, $3 \times 10^6\ M^{-1}\ s^{-1}$ for fum^{2-}, $4 \times 10^5\ M^{-1}\ s^{-1}$ for mal^{2-}, $5 \times 10^6\ M^{-1}\ s^{-1}$ for azobenzene-4,4′-disulfonate, and $8 \times 10^7\ M^{-1}\ s^{-1}$ for diazene.

We have previously shown that the rate constant for self-reaction of diazene is in quantitative agreement with ab initio calculations of a concerted pericyclic transition state for double hydrogen atom transfer.[3,25] An interesting outcome of these calculations was the realization that the potential energy surface is virtually barrierless and that the kinetic barrier is largely entropic. Given this picture of the mechanism, two questions are raised by the slower rates exhibited by the other substrates: do the slower rates still pertain to a concerted mechanism, and, if so, what features of the potential energy surfaces give rise to the slower rates?

In an attempt to address these questions, we have performed ab initio calculations on the reaction of *cis*-N_2H_2 with fum^{2-}, the details of which are presented in Tables S1 and S2 of the supporting information. In the gas phase the molecules form a precursor complex with a free energy of −18.1 kcal/mol. This precursor has C_2 symmetry with the two diazene hydrogen atoms engaged in hydrogen bonding with one oxygen atom each from the two carboxylates. Related precursors have been found in calculations for the reactions with N_2H_2 and C_2H_4,[3] but the stabilization energy is considerable larger in the present case; the difference can be attributed to ion−dipole forces. The transition structure for double hydrogen transfer has C_2 symmetry with the diazene hydrogens synchronously moving toward the olefinic bond. It has an activation free energy of 7.1 kcal/mol relative to the precursor complex. This activation free energy is modestly larger than that calculated for the reactions with N_2H_2 and C_2H_4, perhaps arising from the loss of dipole moment in the N_2H_2 moiety as the system moves to the transition structure. The calculated activation free energy is −11.0 kcal/mol relative to free reactants. Because of the inferred strong electrostatic factors associated with these energies, it is difficult to relate the gas-phase computational results to the aqueous-phase rate constants. The difficulty is highlighted by noting that the experimental rate constants imply a difference of only 2.0 kcal/mol in $\Delta G^‡$ for the two reactions.

In order to account for the electrostatic effects, we performed some calculations of the solvation energies of the various species. The results include the precursor complex with $\Delta G° = -3.3$ kcal/mol, relative to reactants. Compared to the gas-phase calculations, this shows the expected solvent damping of electrostatic effects. Solvation affects the energy of the transition structure to a similar degree, leading to an activation free energy of 5.8 kcal/mol relative to the precursor complex. An activation free energy of 2.5 kcal/mol is calculated relative to the reactants, which is 7.4 kcal/mol *less* than calculated for the reaction with *trans*-N_2H_2. This final result is mildly contrary to the experimental results, where the fumarate reaction has a $\Delta G^‡$ value 2.0 kcal/mol *greater* than for the reaction with *trans*-N_2H_2. This reversal arises from a computed overestimate of 3.3 kcal/mol for the reaction with *trans*-N_2H_2 and a 6.1 kcal/mol underestimate for the reaction with fumarate. We note that these calculations are based on the assumption of equilibrium solvation of the transition state; to the degree that this is not the case, the calculated value of $\Delta G^‡$ will be too low. Correction for this effect should be more significant for the ionic fumarate reaction, and it might invert the relative activation free energies for the two reactions and bring them more into line with experiment.

The above computational results support the notion of a synchronous concerted double hydrogen atom transfer mechanism in the reaction with fum^{2-}, and the numerical results are in reasonable agreement with the rate constants observed. However, the numerical results are not sufficiently refined to explain the relatively small rate differences that we have observed. Thus, the assumption of Garbisch et al. that the relative rates are governed by strain energies remains untested.[13] Further progress will be aided by investigating nonionic substrates and substrates that have even slower reaction rates. It will also be helpful to obtain activation parameters for these reactions. Since these reactions will be slow, the NMR product yield method will be much more effective than the stopped-flow method for determining the requisite data.

(25) Mckee, M. L.; Squillacote, M. E.; Stanbury, D. M. *J. Phys. Chem.* **1993**, *97*, 9074.

(26) Houk, K. N.; Li, Y.; McAllister, M. A.; O'Doherty, G.; Paquette, L. A.; Siebrand, W.; Smedarchina, Z. K. *J. Am. Chem. Soc.* **1994**, *116*, 10895−10913.

In related work, Houk et al. have recently published an analysis of double hydrogen dyotopy in hydrocarbons.[26] These intramolecular double hydrogen atom transfer reactions are close to thermoneutral, unlike the reactions of diazene, and they are quite slow. Houk et al. express some uncertainty as to the degree of synchrony in these reactions. Our calculations on the reaction of diazene with fum^{2-} yield a transition structure that is synchronous, as do our prior calculations on the reactions with *cis*- and *trans*-diazene and with ethylene.[3] For reactions such as those studied by Houk et al., the high synchronous activation enthalpy allows a barrier involving an asynchronous transition structure to become competitive, but in hydrogenation reactions with diazene the synchronous barrier is so low that little is to be gained from an asynchronous transition structure. Of course, the transition *state* can be thought of as an ensemble of trajectories passing through a bottleneck, and even if the transition *structure* is synchronous the majority of the reactive trajectories will be asynchronous. In other words, entropic considerations dictate a degree of asynchrony, even for those reactions having strictly synchronous transition *structures*.

Acknowledgment. This research was supported by a grant from the NSF. D.M.S. is a Sloan Research Fellow.

Appendix

Derivation of Eq 5. Integration of eq 3 leads to eq 5 as follows: Rearrangement of eq 3 gives

$$-dt = \frac{d[N_2H_2]}{2k_{disp}[N_2H_2]^2 + k'_{fum}[N_2H_2]} \tag{A1}$$

The definite integral of this equation is taken from zero time to time t with the corresponding concentrations of $[N_2H_2]$ evolving from $[N_2H_2]_0$ to $[N_2H_2]$, as shown by

$$-\int_0^t dt = \int_{[N_2H_2]_0}^{[N_2H_2]} \frac{d[N_2H_2]}{2k_{disp}[N_2H_2]^2 + k'_{fum}[N_2H_2]} \tag{A2}$$

The right-hand side of this equation is a standard integral with an analytical solution (#37 in the 55th edition of the CRC Handbook of Chemistry and Physics, **1974**, p A-114). Evaluation of this integral gives

$$-t = \frac{1}{k'_{fum}}\left(\ln\frac{[N_2H_2]}{2k_{disp}[N_2H_2] + k'_{fum}} - \ln\frac{[N_2H_2]_0}{2k_{disp}[N_2H_2]_0 + k'_{fum}}\right) \tag{A3}$$

Rearrangement gives

$$-k'_{fum}t = \ln\left(\frac{[N_2H_2](2k_{disp}[N_2H_2]_0 + k'_{fum})}{[N_2H_2]_0(2k_{disp}[N_2H_2] + k'_{fum})}\right) \tag{A4}$$

Exponentiation of the above and further rearrangement gives eq 5.

Derivation of Eq 6. Substitution of eq 5 into eq 4 and rearrangement gives

$$\frac{d[succ]}{dt} = k'_{fum}\left(\frac{k'_{fum}}{\left(\frac{k'_{fum}}{[N_2H_2]_0} + 2k_{disp}\right)e^{k'_{fum}t} - 2k_{disp}}\right) \tag{A5}$$

When this is rearranged and expressed as an integral we obtain

$$\int_{[succ]_0}^{[succ]} d[succ] = (k'_{fum})^2 \int_0^t \frac{dt}{\left(\frac{k'_{fum}}{[N_2H_2]_0} + 2k_{disp}\right)e^{k'_{fum}t} - 2k_{disp}} \tag{A6}$$

The right-hand side of this equation is another standard integral, #526 in the CRC Handbook, and its integration and rearrangement leads to eq 6.

Derivation of Eq 8. Application of the steady-state approximation to eq 2 is accomplished by setting $d[N_2H_2]/dt$ equal to zero, i.e.,

$$0 = k_0'[(NCO_2)_2{}^{2-}]_0e^{-k_0't} - k'_{fum}[N_2H_2]_{ss} - 2k_{disp}[N_2H_2]_{ss}{}^2 \tag{A7}$$

The steady-state concentration of N_2H_2, $[N_2H_2]_{ss}$, is then obtained by applying the quadratic formula and selecting the appropriate root. The result is given as eq 8.

Derivation of Eq 9. Substitution of eq 8 into eq 4 gives

$$\frac{d[succ]}{dt} = k'_{fum}\left(\frac{-k'_{fum} + \sqrt{(k'_{fum})^2 + 8k_{disp}k_0'[(NCO_2)_2{}^{2-}]_0e^{-k_0't}}}{4k_{disp}}\right) \tag{A8}$$

Rearrangement and integration yields

$$\int_{[succ]_0}^{[succ]_\infty} d[succ] = \frac{-k'_{fum}}{4k_{disp}}\int_0^\infty (k'_{fum} - \sqrt{(k'_{fum})^2 + 8k_{disp}k_0'[(NCO_2)_2{}^{2-}]_0e^{-k_0't}})\,dt \tag{A9}$$

Introducing a change of variables such that $Q = e^{-k_0't}$ leads to

$$[succ]_\infty - [succ]_0 = \frac{-k'_{fum}}{4k_{disp}}\int_1^0 \frac{(k'_{fum} - \sqrt{(k'_{fum})^2 + 8k_{disp}k_0'[(NCO_2)_2{}^{2-}]_0Q})}{k_0'Q}\,dQ \tag{A10}$$

Another change of variables such that $U = \{(k'_{fum})^2 + 8k_{disp}[(NCO_2)_2{}^{2-}]_0k_0'Q\}^{1/2}$ leads to

$$[succ]_\infty - [succ]_0 = \frac{-k'_{fum}}{4k_{disp}k_0'}\int_{k'fum}^{[(k'_{fum})^2+8k_{disp}k_0'[(NCO_2)_2{}^{2-}]_0]^{1/2}} \frac{2U}{U + k'_{fum}}\,dU \tag{A11}$$

The right-hand side of this equation is integral #30 in the CRC Handbook, and when evaluated it gives eq 9.

Supporting Information Available: Tables of absolute, relative, and free energies (2 pages). This material is contained in many libraries on microfiche, immediately follows this article in the microfilm version of the journal, can be ordered from the ACS, and can be downloaded from the Internet; see any current masthead page for ordering information and Internet access instructions.

JA951633U